J Neuropathol Exp Neurol
Vol. 68, No. 3
March 2009
pp. 286–299

ORIGINAL ARTICLE

Novel Isolated Cerebral ALλ Amyloid Angiopathy With Widespread Subcortical Distribution and Leukoencephalopathy Due to Atypical Monoclonal Plasma Cell Proliferation, and Terminal Systemic Gammopathy

Roland Schröder, MD, Martina Deckert, MD, and Reinhold P. Linke, MD

Abstract

Neuropathologic and biochemical findings in a 34-year-old man whose disease began 2 years before death appearing as chronic progressive encephalitis and culminated in mutism are reported. Cerebrospinal fluid and serum of the patient showed a brain-restricted monoclonal λ-light chain apparently produced by a small monoclonal immunoglobulin Gλ plasma cell population. In the preterminal stage, there was a systemic monoclonal gammopathy, the source of which could not be identified. At autopsy, there was extensive amyloid deposition in most vessels throughout the cerebral and cerebellar white matter, basal ganglia, and thalamus and diffuse leukoencephalopathy; cerebral and cerebellar cortices, other portions of the CNS, and non-CNS tissues were spared. Partial amino acid sequence analysis demonstrated that the amyloidogenic protein originated from immunoglobulin λ-light chains which were produced by monoclonal plasma cells. There are 2 similar cases reported in the literature. The distribution of ALλ deposits in these 3 cases indicates that widespread subcortical vascular amyloidosis with leukoencephalopathy is a novel clinicopathologic entity distinguished from other cerebral diseases with local amyloid light chain deposition, including amyloidoma, leptomeningeal vascular amyloidosis, solitary intracerebral plasmacytoma, primary intracerebral lymphoma with plasmacytic differentiation, and multiple sclerosis with demyelination-associated amyloid deposition.

Key Words: Amyloid angiopathy, Immunoglobulin λ-light chain–derived amyloid, Leukoencephalopathy, Monoclonal gammopathy, Monoclonal immunoglobulin deposition disease, Plasma cell proliferation, Small-vessel diseases.

INTRODUCTION

Vascular amyloid deposition in the brain (i.e. cerebral amyloid angiopathy [CAA]) is associated with diverse disease processes and results from deposition of a variety of proteins (1–5). One of these reviews indicates that the component peptide of amyloidoma has been identified as amyloid light chain–λ (ALλ) (4) (see Table 1 for nomenclature). In addition to biochemical classification, conditions with CNS amyloid vasculopathy can be separated according to the regional distribution pattern of the amyloid deposits as follows:

1. A hematogenous pattern of deposition occurs in systemic AA and AL amyloidoses. The brain vessels and parenchyma are usually spared with the exception of the choroid plexus and circumventricular structures, which lack a functional blood-brain barrier (6, 7).
2. In most cases of CAA, there is a predominant meningocortical distribution of the vascular amyloid; in very severe cases, CAA can also extend to white matter, basal ganglia, thalamus, or brainstem (8–10). The amyloidogenic proteins in these cases are of Aβ, ATTR, ACys, or APrP type (11), respectively, (Table 1).
3. A diffuse pattern in which the vessels of all structures of both gray and white matter in brain and spinal cord are affected has been reported in cases of AGel (12), ABri (13), and ADan (14); possibly another yet unknown protein fragment may be involved in the case of Shaw (15).
4. In addition to the hematogenous pattern, some hereditary ATTR amyloidoses show deposits in meningeal, cortical, and subependymal vessels; that is, a meningoependymal pattern (16).
5. In a subcortical type, there is predominant involvement of the white matter and partial involvement of central gray structures of the brain by vascular amyloid. Intracerebral amyloidomas that evolve from confluent vascular and perivascular amyloid deposits form a compact mass belong in this category; these amyloidomas are most often located in periventricular and subcortical structures and consist of ALλ-type amyloid (17). Rarely, intracerebral plasmacytoma and low-grade B-cell lymphoma may produce amyloid deposits in deep brain structures; these are also of immunoglobulin light chain origin, as they are in other organs. Another pattern in this group is the amyloid deposition in and around cerebral vessels in multiple sclerosis (MS) lesions; these deposits also consist of ALλ peptides. Amyloid deposition has also been reported to

From the Department of Neuropathology (RS, MD), University Hospital of Cologne; and the Innovation Center of Biochemistry (RPL), amYmed Martinsried/Munich, Germany.
Send correspondence and reprint requests to: Roland Schröder, MD, Department of Neuropathology, University Hospital of Cologne, Kerpener Str, 62, D-50924 Cologne, Germany; E-mail: neuropatho@uni-koeln.de
A supplementary table is available online at http://www.jneuropath.com.

TABLE 1. Nomenclature of Amyloid Types

Amyloid Type	Protein Origin
AA	Amyloid A protein
ALκ, λ	Amyloid of immunoglobulin κ- or λ-light chain origin
AHγ	Amyloid of immunoglobulin γ-heavy chain origin
Aβ	Amyloid β precursor protein (AβPP)
ATTR	Amyloid of transthyretin origin
APrP	Amyloid of prion protein origin
ACys	Amyloid of cystatin C origin
AGel	Amyloid of gelsolin origin
ABri	Amyloid Bri (British) precursor protein
ADan	Amyloid Dan (Danish) precursor protein
$A\beta_2M$	Amyloid of β_2 microglobulin origin
AApo A I	Amyloid of apolipoprotein A I origin
AFib	Amyloid of fibrinogen Aα chain origin

affect most of the vessels throughout the cerebral white matter exclusively (18), but the chemical type of this amyloid is unknown.

The present study examines a previously reported case and focuses on the subcortical amyloid deposition pattern and its associated conditions. We demonstrate by immunohistochemistry and by partial amino acid sequence analysis that the cerebrovascular amyloid in our case is of monoclonal immunoglobulin λ–light chain origin. Together with 2 similar cases of the literature that have not yet been biochemically defined, we propose that this is a distinct disease entity and compare features of these cases with those of other known cerebral AL deposition diseases.

Clinical History

The patient, KAB (a designation unrelated to his name), died at 34 years of age with the clinical diagnosis of chronic encephalitis; clinical details have been reported elsewhere (20). His medical history and his family history were negative for neurologic diseases. He developed generalized tonic-clonic seizures 25 months before death. He also developed a progressive amnestic syndrome with memory loss, aphasia, and a paranoid period. He grew increasingly apathetic and developed spastic quadriplegia, and for the last 5 months of life, he persisted in a state of akinetic mutism with a vegetative state. Multiple electroencephalogram examinations showed general flattening with bitemporal dysrhythmia that progressed during the disease course. Contrast-enhanced computed tomographic scans in the last 5 months demonstrated slight enlargement of the ventricles; focal lesions were not identified.

Several cerebrospinal fluid (CSF) examinations showed total protein of 48 to 105 mg/dl and local production of immunoglobulin (Ig) G (26% to 76% of total CSF-IgG), but not of IgA or IgM, as determined by comparison of CSF and serum IgG and albumin concentrations. This CSF-restricted IgG production tended to decrease during the disease course. Cell counts were normal, with only small lymphocytes and monocytes (20). Other studies of blood and serum were unremarkable and included lack of evidence of inflammatory or immunologic disorders, including measurements of antinuclear and anti-mitochondrial antibodies. There was no hypergammaglobulinemia. The search for infectious agents in serum and CSF was negative, including syphilis, borreliosis, brucellosis, fungi, herpes simplex, varicella zoster, rubella, measles, cytomegalovirus, parainfluenza 1–3, mononucleosis, ornithosis, adenoviruses, Coxsackie viruses, lymphocytic choriomeningitis virus, central European encephalitis virus, mycoplasma, leptospirosis, cysticercosis, echinococcosis, and toxoplasmosis. Similarly, no viral etiology could be identified after cell culture of and inoculation of neonatal mice with postmortem brain samples.

MATERIAL AND METHODS

Histology and Immunohistochemistry

Paraffin sections of 5- to 10-μm thickness from all portions of the formalin-fixed brain and spinal cord were routinely stained with hematoxylin and eosin, Cresyl violet, Luxol fast blue, and Congo red (CR) (21) stains. Representative regions were additionally stained with periodic acid Schiff, iron stain, Van Gieson, Ladewig Trichrome, Campbell (amyloid), Gallyas (tangles), Palmgren (axons), Gordon (reticulin fibers) and Holzer (astroglial fibers) preparations. Sections from all peripheral organs were also stained with hematoxylin and eosin and CR stains of one representative tissue block colloidal iron reaction for acid groups (Hale), Alcian blue (pH 5.8) at 2 critical electrolyte concentrations for proof of highly sulfated polysaccharides (22), and Toluidine blue (metachromasia) stains were used.

For immunohistochemistry, primary antibodies against the following antigens were applied on paraffin sections using the avidin-biotin complex technique with 3,3′-diaminobenzidine as chromogen partly after heating or enzyme pretreatment for antigen retrieval: glial fibrillary acidic protein (polyclonal, 1:3000; Dako, Hamburg, Germany), neurofilament (1:200; Dako), β-amyloid precursor protein (1:200; Zymed, South San Francisco, CA), laminin (1:50; Dako), smooth muscle actin (1:100; BioGenex, San Ramon, CA), CD3 (polyclonal, 1:100; Dako), CD4 (1:40; DCS Innovative Diagnostik-Systeme, Hamburg, Germany), CD8 (1:50; Dako), CD20 (1:100; BioGenex), CD25 (1:25; Novocastra Laboratories, Newcastle upon Tyne, UK), CD68 (1:100; Dako), human leukocyte antigen-DR (1:50; Dako); CD138 (1:100; Biozol, Kidlington, Oxford, UK), p 63-VS38C (1:100; Dako), κ-light chains (1:1000; Zymed), λ-light chains (1:800; BioGenex), IgA (1:100; Dako), IgG (1:100; Dako), IgM (1:100; Dako), and MIB-1 (1:300; DCS); additionally, monoclonal Pan-Aβ (synthetic residues 8–17, 1:50; Dako) was applied after concentrated formic acid pretreatment. Evaluation included appropriate positive and negative controls. Counting of labeled cells was performed on serial sections within the same representative area.

Electron Microscopy

Small pieces of tissue were excised from a representative paraffin block, deparaffinized, and postfixed in buffered glutaraldehyde, followed by 1% OsO_4. The specimens were

dehydrated in graded ethanol and reembedded in Epon. For histologic controls, semithin sections stained with Toluidine blue were used. Ultrathin sections stained with 1% uranyl acetate, and lead citrate were examined with an electron microscope (Philips EM 400).

Diagnosis and Classification of the Amyloid

Amyloid was diagnosed by congophilia and green birefringence under polarized light (21) and by the more sensitive CR fluorescence technique (23, 24). The immunohistochemical classification was performed on representative paraffin sections using the peroxidase antiperoxidase technique with H_2O_2 as substrate and 3-amino-9-ethylcarbazole as chromogen, as previously described (24). The anti-amyloid antibodies used for amyloid typing on formalin-fixed and paraffin-embedded tissue sections were provided by amYmed (Martinsried, Germany). Pretreatment of the sections with 15% formic acid was used for the anti-Aβ and anti-PrP but not the other antibodies. The specificity of these antibodies has been verified on a larger series of prototype amyloids by their application on hundreds of samples submitted for routine amyloid typing (24, 25).

The following primary antibodies directed against human amyloid proteins or respective peptides (immunogen listed in Table 2) were used: murine monoclonal anti-AA (mc 1; amYmed product code, Y110; 1:10); rabbit polyclonal antibodies as ALλ (HAR; code, Y120; 1:2000), ALλ (ULI/LAT; code, Y130+1; 1:1000), ALκ (SIN; code, Y140; 1:1000), ALκ (KRA/KUN; code, Y150+1; 1:2000), ATTR (TIE; code, Y180; 1:1000), Aβ (SIZ; code, Y260; 1:800), APrP (code, Y270; 1:1000), ACys (code, Y 220: 1:1000), $A\beta_2M$ (WOE; code, Y170; 1:1000), AFib Aα (code, Y190; 1:1500), AHγ (SOL; code, Y160;1:1000), AApoA-I (code, Y200; 1:500), and AGel (code, Y230; 1:300). Specificity of the immunohistochemical reactions was determined using positive controls that included a section containing the respective amyloid for each antibody; negative controls were used in every set of examinations, as published (24, 25). The evaluation was performed in a blinded manner.

TABLE 2. Immunohistochemical Staining With Anti-Amyloid Antibodies

Antibody	Immunogen*	Control†	A (KAB)‡	Consistency§
Anti-AA (mc 1)	A	+++	0	
Anti-ALλ (HAR)	A	+++	++ - +++	C
Anti-ALλ (ULI/LAT)	A	+++	++	C
Anti-ALκ (SIN)	A	+++	0 - ++	IC
Anti-ALκ (KRA/KUN)	A	+++	0 - +	IC
Anti-Aβ (SIZ)	A	++	0	
Anti-ATTR (TIE)	A	+++	0 - +	IC
Anti-AHγ (SOL)	A	+++	0	
Anti-$A\beta_2M$ (WOE)	A	++	0	
Anti-PrP	SP	+++	0	
Anti-Apo AI	SP	++	0	
Anti-Gel	SP	++	0	
Anti-Fib Aα	P	+++	0	
Anti-Cys C	P	+++	0 - +	IC

*Immunogen: A, amyloid peptide; P, natural protein or fragment thereof; SP, synthetic peptide.

†Reaction intensity of the positive control of the chemically analyzed amyloid protein (0, no reaction; +, moderate reaction; ++, strong reaction; +++, very strong reaction).

‡Reaction intensity of amyloid KAB.

§C, consistent staining; IC, inconsistent.

Partial Amino Acid Sequence Analysis of the Amyloid Protein

A fresh-frozen tissue sample of the left temporal lobe from the autopsy brain (kindly provided by Prof. Ackermann, Cologne, Germany) was water-extracted using the micro-extraction procedure (26), reduced in 0.1 mol/L of βME for 1 hour in PBS, flushed with N_2, and alkylated by adding iodoacetamide as a powder to result in a concentration of 0.2 mol/L for 1 hour; both were agitated. After sufficient dialysis against doubly distilled water and lyophilization, the dry powder was separated by 10% sodium dodecyl-polyacrylamide gel electrophoresis, according to Reference 27. The separate proteins were either stained with Coomassie blue or electrotransferred onto a nitrocellulose membrane (B86, Schleicher & Schüll, Dassel, Germany). The membrane-bound proteins were probed with anti-ALλ (HAR, amYmed) in Western blotting, as described (28). Because automated N-terminal amino acid sequence of major low molecular proteins did not yield relevant N-terminus, in-gel digestion was performed using restriction endoproteinases. The resulting peptides were separated, and the N-terminal amino acid sequence was determined by automated Edman degradation (29).

Quantification of Free Ig Light Chains in CSF and Serum

Three paired samples of lumbar CSF and serum were available from Prof. Ackermann. Each pair was taken from the patient on the same day 13.6, 18.6, and 23.9 months after disease onset; the last was 1.2 months before his death. The 1.0- to 1.5-ml samples had been kept at −20°C for more than 20 years. The concentrations of the free immunoglobulin light chains κ and λ were determined in all samples using a commercial kit (The Binding Site, Schwetzingen, Germany, by courtesy of Dr. Zorn, Heidelberg, Germany).

Isoelectric Focusing, Electrotransfer, and Immunodetection

Only sufficient quantities from the last CSF/serum samples were available for this analysis. Isoelectric focusing was performed on 9 × 12-cm glass plates with a semisolid carrier of 10 ml. The carrier consisted of 0.9% isoelectric focusing (charge free) agarose (Pharmacia, Uppsala, Sweden) and 5% polyacrylamide and 0.25 ml of 40% ampholine (pH 3.5 to 10; Pharmacia). The 0.2- to 1-mg samples were dissolved in 20-μl 4-mol/L of urea in water and run on constant of 8 W for 90 minutes with 0.5 mol/L acetic acid in water as anode solution and 1 mol/L of NaOH as cathode solution. The proteins were fixed in 3.5% sulfosalicylic acid and 5% trichloroacetic acid in 33% methanol in water for 30 minutes. After washing in water for 10 minutes, the carrier was dehydrated with cellulose filter sheets under 1 kg of

pressure. The air-dried plates were then stained with 0.1% Coomassie brilliant blue 250 R in methanol (20%), acetic acid (10%) in distilled water for 3 minutes, and destained in the same solvent lacking 250 R until the background became clear.

The separated proteins were then either stained with Coomassie blue or analyzed immunochemically after electrotransfer onto nitrocellulose (B 86 membrane, Schleicher & Schüll), as described (28). The membrane-fixed proteins were then probed for the presence of κ- and λ-light chains using anti-κ and anti-λ antibodies (prepared in rabbits against Bence-Jones proteins isolated from human urine in the amYmed laboratory) and using the peroxidase antiperoxidase system.

RESULTS

General Autopsy

The viscera of patient KAB did not show substantial abnormalities. Histologically, in the liver, spleen, kidney, heart, lung, pancreas, adrenal, thyroid gland, prostate, testis, bone marrow, lymph nodes, skeletal musculature, and peripheral nerves, no amyloid could be detected using CR/birefringence and the more sensitive CR fluorescence method. The bone marrow and the spleen did not show an increase in lymphoid or plasma cells. The cause of death was a recent massive hemorrhage into the right cerebellar hemisphere, probably secondary to the vasculopathy described in the succeeding sentences and terminal anticoagulation for the prevention of thrombosis.

Neuropathology

Gross Examination

The brain was swollen and weighed 1,700 g; it showed soft large arteries and appeared slightly atrophic in the frontoparietal region. The ventricles were moderately dilated. Coronal slices exhibited numerous tiny, sometimes gray, apparently vessel-associated spots causing a stubble-like roughness on the cut surface by their firm quality; these were symmetrically distributed within the cerebral white matter and thalamus.

Perivascular Amyloid Deposition

In large histologic sections, there was an enormous number of small vessel–associated foci in a symmetrical distribution mainly throughout the white matter of all cerebral lobes, internal capsule, basal ganglia, thalamus, amygdala, cerebellar white matter, and dentate nucleus, clearly slighter in midbrain, pons, medulla oblongata, and only occasionally in the spinal cord (Fig. 1). In addition to the cerebral white matter, the most severely affected area was the mediodorsal nucleus of thalamus. Arteries with luminal diameters up to 250 μm, arterioles, capillaries, and venules had perivascular deposits of a homogenous, eosinophilic, periodic acid Schiff positive, and argentophilic substance that gave a strong CR reaction with green birefringence and intense orange-red CR fluorescence typical of amyloid (Fig. 2A–F). All vessels in many areas were thickened by these deposits; the deposition sometimes resulted in a narrowing or occlusion of capillary lumens. There were compact amyloid precipitation in the vessel walls with less intensely congophilic, comblike bundles that protruded outside of the external surfaces of the smooth muscle cells into the perivascular spaces of arteries and arterioles and outside of the basement membrane of capillaries and venules into the adjacent parenchyma (Fig. 2C). Confluent intraparenchymal amyloid masses occasionally reached diameters of up to 4 mm. Because of their increased thickness, the very prominent vessels gave the impression of a quantitatively increased vascularization, but a comparison of vessel counts

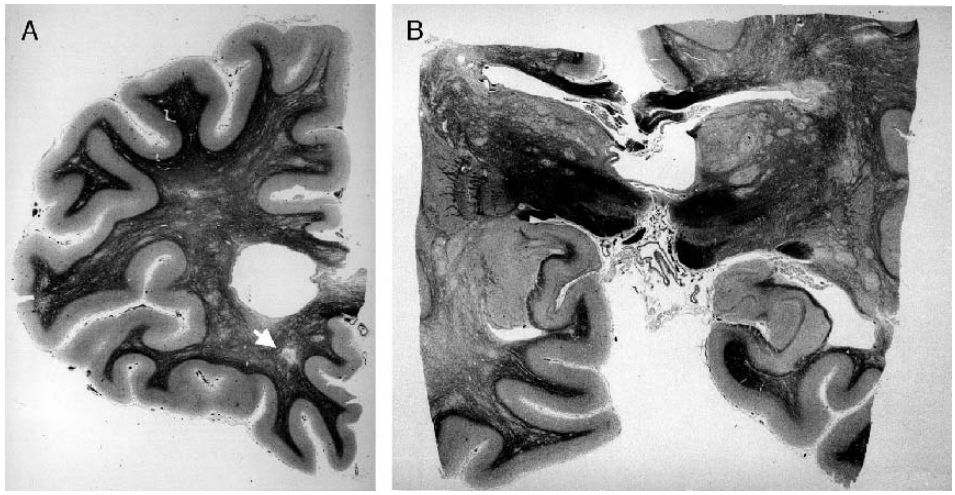

FIGURE 1. Sections through the frontal lobe **(A)** and the central ganglia **(B)** demonstrate severe subcortical angiopathy and leukoencephalopathy. Myelin stains show multiple light spots in all white matter areas and the thalamus and diffuse demyelination with better preservation of subcortical fibers, corpus callosum, optic tract, and midbrain. The cerebral cortex is not involved. There is a single area of necrosis in the basis of the gyrus rectus (**A**, arrow). Luxol fast blue stain.

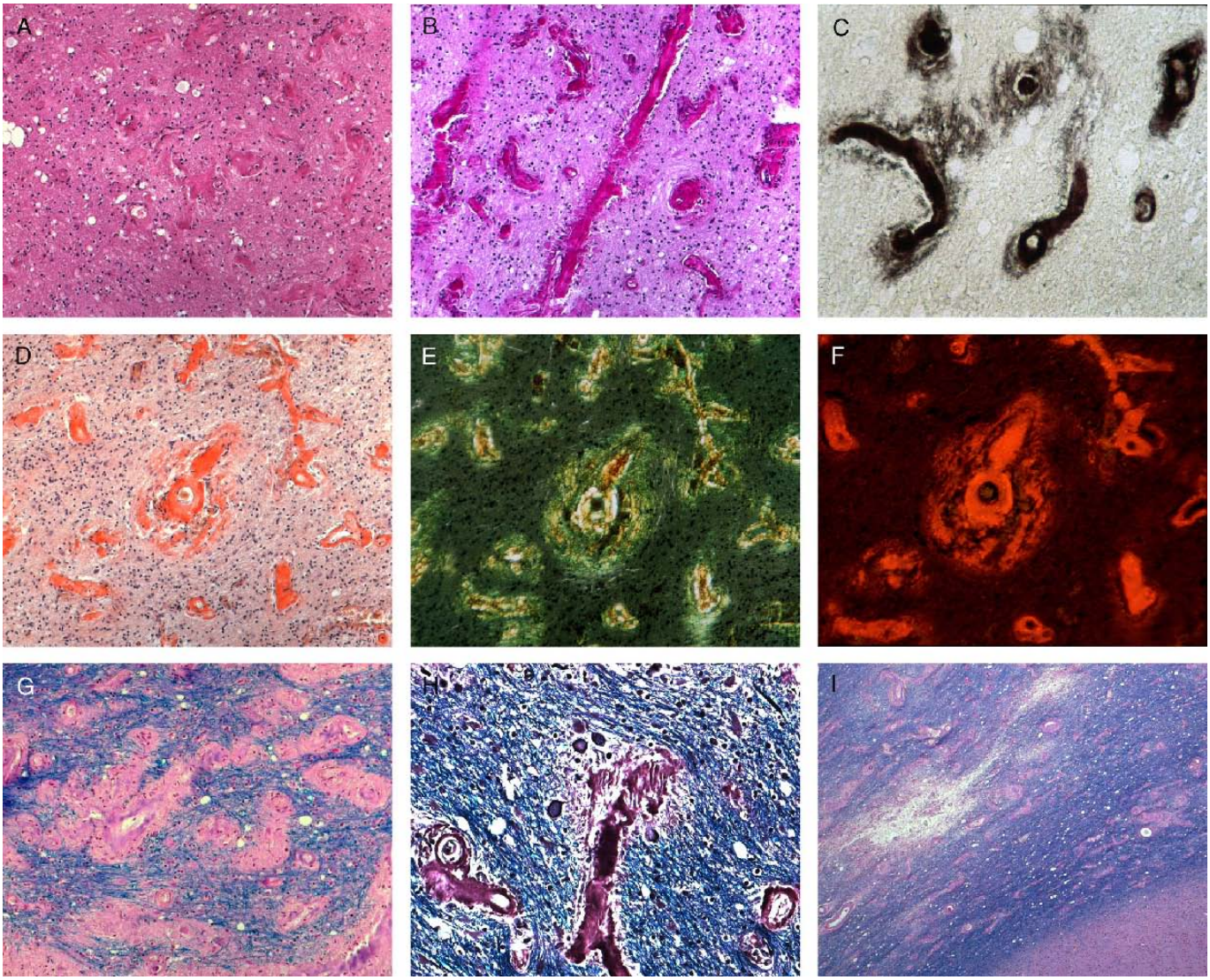

FIGURE 2. Histologic features of amyloid deposits in cerebral white matter. **(A)** Microvessel-bound eosinophilic amyloid in white matter. Hematoxylin and eosin, 150×. **(B)** Strong periodic acid Schiff staining of amyloid deposits involving partly obliterated small vessels. Periodic acid Schiff, 150×. **(C)** Silver impregnation of the amyloid substance at the capillaries; the periphery of the precipitates sometimes show brushlike or comblike patterns. Campbell, 370×. **(D–F)** Congo Red (CR) stain **(D)**, yellow-green birefringence under polarized light **(E)**, and CR fluorescence of the vessel-associated amyloid in the same area **(F)**. 150×. **(G)** Perivascular amyloid deposits (light red) displace the myelinated fibers (blue). Luxol fast blue/Nuclear fast red, 150×. **(H)** Silver-impregnated axon balls (black and dark gray) in a perivascular area with loose amyloid deposition (brown) and demyelination. Palmgren/Luxol fast blue, 300×. **(I)** Old microinfarct in the white matter between massively altered vessels. Uninvolved cortex is seen in the lower right corner. Luxol fast blue/Nuclear fast red, 50×.

with normal control cases did not confirm this. The cerebral and cerebellar cortical vessels were strikingly free of amyloid (Fig. 3); only a few sporadic vessels in the lower layers of the cortex were involved. Amyloid deposits were also observed but in only small amounts in some leptomeningeal vessels (Fig. 3); they appeared also as circumscribed starlike precipitates on strands of connective tissue in the subarachnoid space, particularly in the cerebellar and spinal regions (Fig. 4I). The proximal spinal nerve root vessels also contained amyloid that stopped at the site of transition of the nerve through the dura mater; thus, no amyloid was detected outside the arachnoid coverings in any part of the body. Only a few larger arteries at the insertion line of the choroid plexus were affected, whereas the area postrema and infundibulum of the hypophysis (i.e. typical sites of hematogenic amyloid accumulation in brain in systemic AA and AL amyloidosis) were spared.

Very few iron-containing macrophages were found around isolated affected vessels, indicating previous microhemorrhages. All amyloid deposits gave strong histochemical

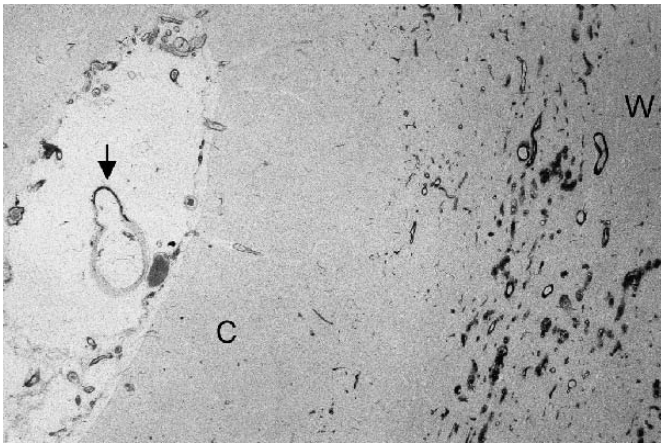

FIGURE 3. Silver stain demonstrates the typical subcortical distribution pattern of the amyloid depositions (black) involving nearly every vessel in the white matter (W) and sparing the cerebral cortex (C). There is only focal involvement of a single meningeal artery (arrow). Campbell preparation, 12×.

reactions for acid groups and showed the presence of highly sulfated polysaccharides through preserved, although reduced, staining at the high electrolyte concentration.

Parenchymal Destruction

Myelin stains demonstrated widespread diffuse symmetric demyelination of the cerebral (Fig. 1A, B) and cerebellar hemispheres with some reduction of myelinated fibers between affected vessels; in some places, this progressed to subtotal focal necroses in subcortical and deep white matter (Figs. 1A, 2I), thalamus, caudate nucleus, and amygdala. There was also displacement of the myelinated fibers by the vascular amyloid deposits and partial demyelination of adjacent fibers with resting naked axons and (β-amyloid precursor protein–positive) axon balls in small rims (Fig. 2G, H and not shown). The intensity of all these alterations seemed to correlate with the severity of the amyloid accumulation at the small vessels. Additionally, in the white matter, there were a few microfoci of calcified dystrophic axons. As a result of all of these symmetric lesions, there was secondary degeneration of both corticospinal tracts from the internal capsule downward to the spinal cord. The midbrain, medulla oblongata, and spinal cord were largely preserved.

Isolated amyloid deposits showed associated multinucleated foreign body giant cells that probably were degrading amyloid. Apart from some amyloid-associated macrophages and very few lymphocytes and plasma cells—the latter with sporadic Russell bodies (i.e. morula cells)—there was no clear evidence of a primary inflammatory process that contributed to the massive amyloid formation around nearly each vessel. No viral inclusion bodies were detected. Neuritic plaques and neurofibrillary tangles were not present.

There was diffuse astrocytosis in the white matter and in the affected central gray matter that was accentuated around arterioles and showed strong glial fibrillary acidic protein immunostaining of the hypertrophied cells; their astrocyte processes formed a tiny network around the amyloid deposits (Fig. 4A) and were sometimes intermingled with the peripheral brushlike borders of the deposits. This corresponded to the demyelinated rim. Activated astrocytes were also seen in subpial areas, and in the white matter, they occasionally contained multiple micronuclei or an enlarged lobulated nucleus with nucleolus (i.e. "Creutzfeldt cells"), as seen in some inflammatory diseases and cerebrovascular disorders (30).

Lymphocytes and Monotypic λ-Light Chains Producing Plasma Cells

Infiltrating cells were analyzed using a panel of antibodies and semiquantitatively evaluated to determine their relative frequencies (Table 3). $CD3^+$ T cells showed a perivascular accentuation but rather diffuse distribution and consisted nearly exclusively of $CD8^+$ cytotoxic cells (Fig. 4B). $CD4^+$ T cells and $CD25^+$ activated T cells were very scarce; likewise, $CD20^+$ B lymphocytes were found in small amounts (Fig. 4C). In contrast, several plasma cells were identified and occurred in characteristic intimate contact with the amyloid, sometimes within peripheral parts of the deposits; this contact was associated with round and often bipolar cell forms (Fig. 4E). These cells showed a cytoplasmic reaction with anti-λ (Fig. 4F) and with anti-IgG, but not with anti-κ, anti-IgM, and anti-IgA. Single plasma cells showing this IgG,λ immunoreactivity were also found in the subarachnoid space along with $CD8^+$ T cells and macrophages. Activated $CD68^+$ and human leukocyte antigen–DR^+ microglia/macrophages were observed in higher amounts around and within the amyloid deposits and represented the bulk of the perivascular cell accumulation (Fig. 4D). They were also diffusely distributed in the parenchyma and accumulated in focal necroses. Quantitatively, these microglia/macrophages were the most numerous cells identified. Other types of infiltrating cells were present in distinctly fewer numbers (Table 3). Likewise, the overwhelming of plasma cells over mature β-lymphocytes was striking. Approximately 3% of the plasma cells showed proliferation (MIB-1 labeling, not shown).

Electron Microscopy

By electron microscopy, the amyloid deposits consisted of extracellular straight, nonbranching fibrils of 7 to 10 nm in thickness (data not shown). In the inner compact parts, they were often tangentially oriented around the vessel circumference, sometimes intermingled with collagen fibers; in the abluminal parts, they were loosely and randomly arranged, and in the fringe-like borders, they were more radially oriented. At the rim, they were in intimate contact with filament-rich astroglial processes, myelinated, and demyelinated axons. Single plasma cells were observed in this marginal contact zone.

Immunohistochemical Identification of the Amyloid Class

Because no Pan-Aβ reactivity of the amyloid was found, we tested using our anti-amyloid antibody panel. Of

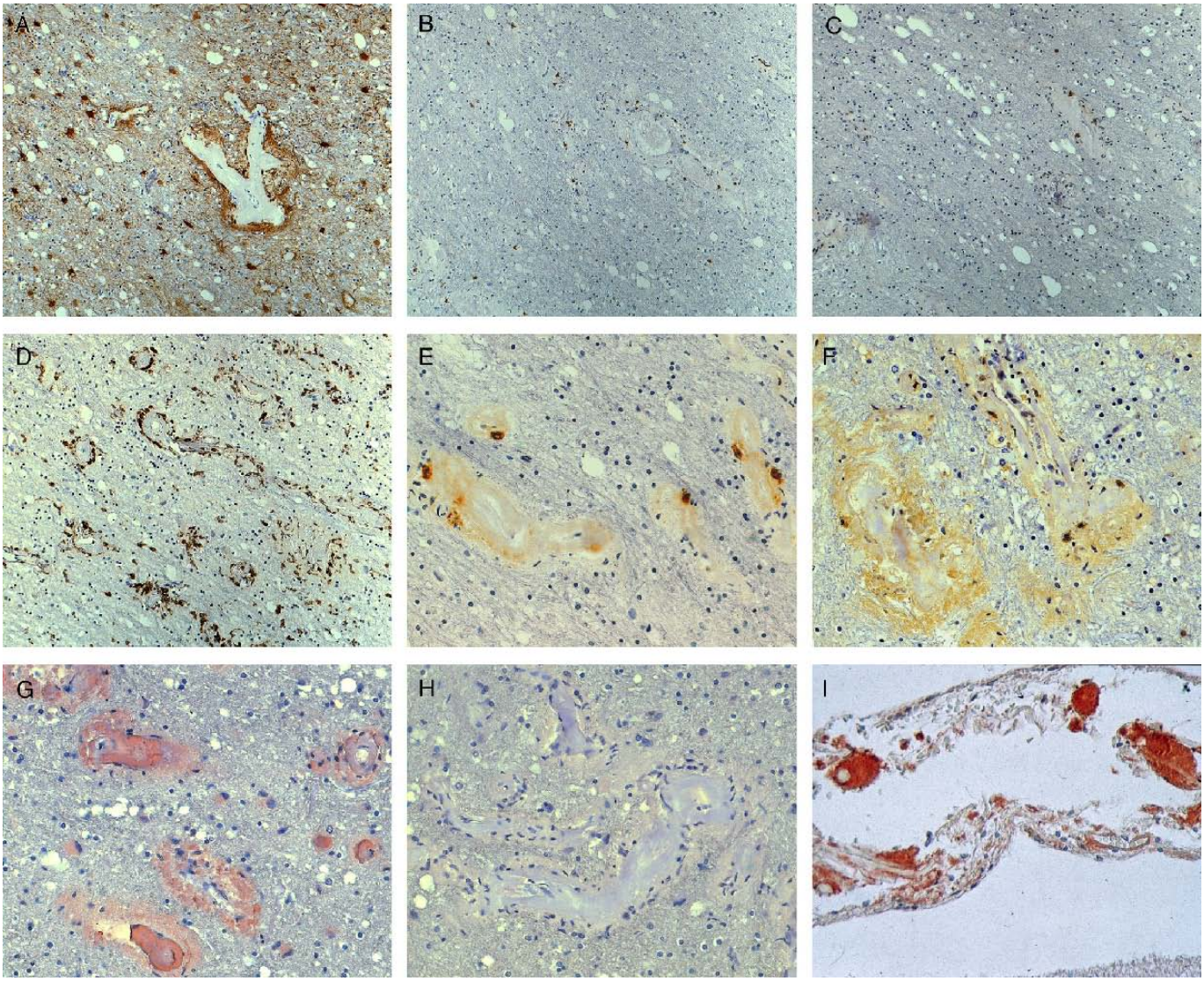

FIGURE 4. Immunohistochemistry of amyloid deposition and cellular reactions. **(A)** Astroglial reaction with hypertrophic cells and periarteriolar fine astroglial network of cell processes. Glial fibrillary acidic protein, 150×. **(B)** Diffuse parenchymal infiltration of CD8 T cells. CD8, 150×. **(C)** Few mature B cells are associated with the vessels. CD20, 150×. **(D)** Macrophage accumulation around the vascular amyloid deposits and within the white matter. CD68, 150×. **(E)** Plasma cells closely apposed to amyloid deposits. CD138, 300×. **(F)** Plasma cells strongly react with anti-λ antibody; there is distinct but slight staining of the amyloid complexes. λ, 300×. **(G)** Strong reaction of the amyloid deposits with anti-ALλ antibody. ALλ (HAR), 300×. **(H)** Control reaction with the anti-Aβ antibody does not show any immunostaining of the amyloid. Aβ (SIZ), 300×. **(I)** ALλ staining of subarachnoid deposits in the spinal region. ALλ (HAR), 300×. All are slightly counterstained with hemalum.

14 antibodies, only the 2 directed against ALλ amyloid proteins showed strong and consistent reactivity with the amyloid deposits (Fig. 4G, I). In contrast, the antibodies directed against the native λ-light chains gave a weaker staining (Fig. 4F). However, the other 12 antibodies, specifically for different amyloid proteins, including anti-Aβ (SIZ) (Fig. 4H), reacted either weakly and/or inconsistently or not at all according to previously published criteria (24) (Table 2). Thus, this cerebrovascular amyloid was classified as of the ALλ type.

Similarly, the mature-appearing plasma cells showed cytoplasmic immunoreactivity with our 3 λ- but not our 3 κ-reagents. In conjunction with the amyloid class findings, this strongly indicates monoclonality of the plasma cells. Direct confirmation of monoclonality by polymerase chain reaction–based rearrangement analysis was not possible because the DNA was destroyed.

The hypertrophied astrocytes often also showed intense binding of antibodies against ATTR and ACys as well as those against λ-light chains, IgG, IgM, neurofilament, and smooth muscle actin. This frequent cross-reactivity pattern may partly be the result of active resorption of protein from the extracellular space or possible imbibition in early autolysis.

TABLE 3. Composition of Leukocytic Infiltrates in the Subcortical White Matter of the Frontal Lobe

Antigen	Cell Specificity	Cells/mm^2*
CD3	T cells	32.0
CD8	Cytotoxic T cells	32.3
CD4	Helper T cells	0.7
CD25	Activated T cells	2.5
CD20	B cells	2.1
CD138	Plasma cells	13.6
P63-VS38C	Plasma cells	11.1
λ-light chains	Plasma cells	6.5
κ-light chains	Plasma cells	0.0
IgG	Plasma cells	8.7
CD68	Microglia/macrophages	284.9

*Immunostained cells were counted in serial sections of the same representative area of 5 to 10 mm^2. Data shown represent the absolute numbers of the respective cell population per square millimeter.

Biochemical Identification of Amyloid Protein and Proof of Monoclonality

Chemical analysis by amino acid sequencing of a single peptide derived from the purified amyloid protein KAB resulted in the sequence DVGFRNYVSWY, an endekapeptide from the variable region spanning the amino acids 28 to 38 of a human $V\lambda_{II}$ immunoglobulin light chain. This peptide is part of the hypervariable complementary-determining region 1 of the Vλ-chain. The amino acid sequence of the standard $V\lambda_{II}$-protein was taken from the Swiss-Prot P01 706, which published the respective amino acid sequence (31). The identification of a single amino acid sequence of this peptide indicates that this amyloid protein is derived from a monoclonal plasma cell population. The results of the full amino acid sequence analysis will be published separately (manuscript in preparation).

Free Monoclonal λ-Chain and Monoclonal IgG, λ-Chain in CSF and Serum

The clonal pattern of a free immunoglobulin λ-light chain is shown in Figure 5. Monoclonality is indicated by the ladder of a series of equidistant λ-chains in Position 1 A and by the absence of κ-reactivity at the same position in 1 B (Fig. 5). This conclusion is further supported by the position of minor reactivities of traces of normal IgG in Positions 2A and 2B and normal IgG in positions 4A and 4B. In addition to the free λ-chain, the patient's CSF showed also monoclonal IgG, λ proteins of restricted heterogeneity as detected not only by the λ-reactivity seen in 1A with absence of the respective κ-reactivity in 5, 6, and 7 compared with normal proteins (CSF 2A, 2B, and normal serum 4A, 4B), but also by the sole γ-reactivity of the bands in 6 and 7; α- and μ-reactivities were nearly absent (not shown). No monoclonality was seen in normal CSF and serum control samples using the same reagents (6 and 7 in 3B, 4A, and 4B). In particular, the almost identical very slow monoclonal γ-band is clearly visible in the patient's CSF and serum (Positions 1A and 3A) compared with the polyclonal antibodies seen in 3B and 4B, which lack this very slow protein. These data show the presence of monoclonal proteins not only in the CSF but also in the serum samples, both of which were taken approximately 1 month before the patient's death.

Quantitative examination of the 2 free light chains κ and λ revealed decreasing free λ-light chain concentrations during the last 11 months of the disease course but constant normal levels of κ-light chains in the CSF (Fig. 6). In contrast, normal levels of both light chains were found in serum samples over a long period, with a sudden marked increase of free λ-light chains 1 month before death.

DISCUSSION

Patient KAB had a 2-year course of what seemed to be chronic progressive encephalitis and was found at autopsy to have a leukoencephalopathy with central gray matter destruction caused by widespread subcortical amyloid angiopathy without systemic disease. The amyloid was of $ALV\lambda_{II}$-type and originated from a monoclonal immunoglobulin λ-light chain that was present in premortem CSF samples. This monoclonal λ-light chain was produced by a local plasma cell clone that apparently became generalized shortly before his death.

Clinical and Neuropathologic Features

To our knowledge, only 2 similar cases have been reported. Both were published in German and are presented in detail here. In 1949, Peters described a 28-year-old man who died after a 6-year course of progressive dementia with

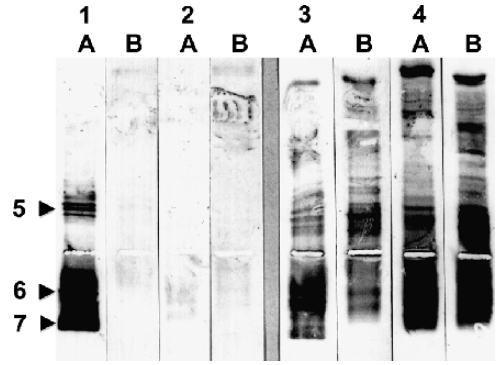

FIGURE 5. Monoclonal proteins in preterminal cerebrospinal fluid (CSF) and serum. Identification of monoclonal immunoglobulin proteins in the patient's cerebrospinal fluid (CSF; 1 A) and in his serum (3 A) was achieved using isoelectric focussing and immunoblotting with anti-λ antibodies. Characteristic proteins seen in the β-region of CSF (1 A) and serum (3 A) represent the free monoclonal (and amyloidogenic) light chains (5, arrowhead). Proteins detected in CSF and serum in the γ-region (6) and in the very slow γ-region (7) represent 2 charge variants of the monoclonal IgG, λ as detected here only with the anti-λ antibodies. These immunochemical reactions were controlled using anti-κ antibodies on the patient's CSF (2 A) and serum (4 A) with no detection of monoclonal protein. The antigen control included normal CSF (1 B) and normal serum (3 B) examined with anti-λ antibodies and the same antigens examined with the anti-κ antibodies in 2 B (normal CSF) and 4 B (normal serum).

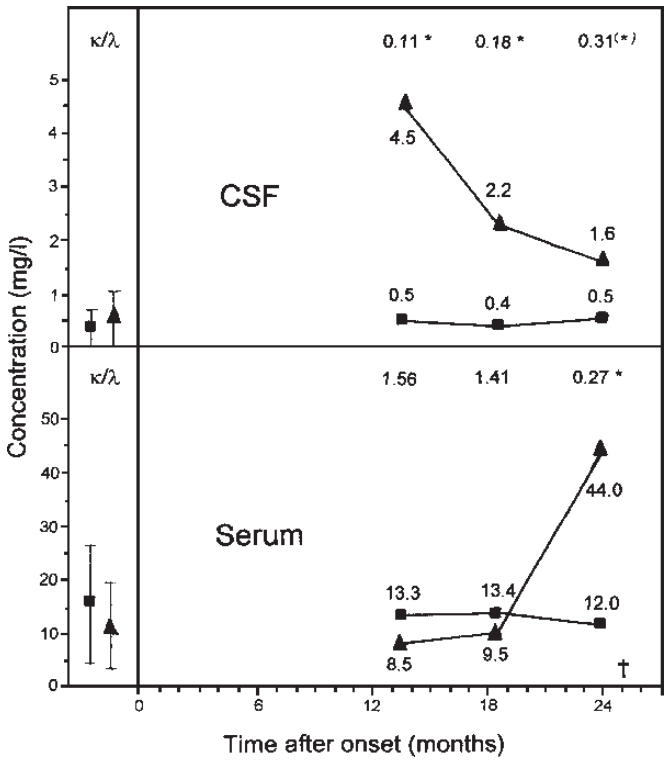

FIGURE 6. Free light chain concentration (in milligrams per liter) of λ-light chains (▲) and of κ-light chains (■) in cerebrospinal fluid (CSF) and serum of patient KAB during the latter course of the disease. (†, death at 25 months). The κ/λ-values marked with asterisks are statistically significant beyond the normal limits and indicate the presence of a monoclonal λ-light chain. Normal values (left panels) in the CSF were 0.4 (range, <0.7) mg/L for κ and 0.6 (range, <1.1) mg/L for λ; in the serum, they were 16.0 (range, 5.7–26.3) mg/L for κ and 11.4 (range, 3.3–19.4) mg/L for λ.

paranoid episodes, cerebellar signs, spastic paresis, blindness, and final stupor. Cerebrospinal fluid showed a slight elevation of protein with inflammatory colloidal (normomastix) and gold sol tests and a normal cell count; atypical MS was diagnosed (18, 19). The patient died with severe malnutrition and bronchopneumonia. At autopsy, widespread vascular amyloid deposits were restricted to the brain; the deposits were symmetrically distributed in the white matter of cerebrum, cerebellum, and medulla oblongata, with only rare spread to lower cerebral and cerebellar cortical layers. Basal ganglia, diencephalon, spinal cord, meningeal, and choroid plexus vessels were uninvolved. There was diffuse cerebral demyelination with secondary pyramidal tract degeneration but no evidence of MS. Some subcortical white matter vessels that lacked amyloid deposits were surrounded by tight plasma cell accumulations, often with Russell bodies. A possible role for these plasma cell infiltrates in the amyloid formation was suggested; archival blocks are not available.

The second case (designated DU 1) was initially published as an abstract by Gerhard (32) and later described in more detail by Yuan (33, case II). This 55-year-old man developed dementia accompanied by ataxia, tremor, and spastic paresis and died after 1 year from a pulmonary embolism in a cachectic state. Cerebrospinal fluid showed a slightly elevated cell count and protein, and an inflammatory normomastix reaction and the clinical diagnosis was MS. Autopsy did not reveal systemic amyloidosis. There were extensive vascular amyloid deposits in brain distributed throughout all lobes of the cerebral and cerebellar white matter, with confluence in the periventricular region of the lateral ventricles leaving islands of intact parenchyma and spreading to the basal ganglia and thalamus. Cerebral and cerebellar cortex, leptomeninges, midbrain, medulla, and spinal cord were uninvolved. There was diffuse demyelination in the white matter of cerebrum and cerebellum and optic nerve and occasional microinfarcts. There was secondary degeneration of the fornix and pyramidal tracts. Single-foreign-body giant cells, macrophages, lymphocytes, and plasma cells, the latter occasionally with Russell bodies, were present around vessels both with and without amyloid accumulations. Because plasma cells showed λ-restriction and the amyloid showed stronger λ- than κ-light chain immunoreactivity, ALλ amyloid formation by a monoclonal plasma cell population was suggested. Our subsequent examination (courtesy of Prof. Gerhard, Essen, Germany) with our panel of anti-amyloid antibodies confirmed ALλ amyloid deposition (Supplementary Table), as found in our patient KAB.

These 3 cases developed a more or less rapidly progressive amnestic syndrome accompanied by cerebellar signs and central paresis, also partly with generalized seizures, fatal deterioration to akinetic mutism, and CSF alterations, the latter earlier exclusively interpreted as suggesting an inflammatory process. The clinical courses are similar and are not typical of MS. The cases show uniformity in the conspicuous distribution pattern of extensive vessel-bound amyloid formation through the entire cerebral and cerebellar white matter with a tendency to an additional involvement of deep gray nuclei, but leaving the cerebral and cerebellar cortices nearly completely intact. This subcortical pattern is distinct from all other known diseases with CAA.

The angiopathy was associated with diffuse demyelination that occasionally developed into subtotally demyelinated and focally necrotic lesions and severe leukoencephalopathy. Their cause was most likely a perfusion disturbance as a result of the rigidity of affected microvessels or hypoxia resulting from impaired diffusion by the masses of the deposited material; chronic edema as a consequence of blood-brain barrier disruption may also have played a role. As in case KAB, perivascular demyelination and axonal injury may also be present in amyloidoma of the brain (34, 35). This might be caused by neurotoxic effects of substances released through a functionally defective vascular wall, direct effects of the amyloid, the λ-light chains or their oligomers, or blockage of perivascular drainage pathways by the amyloid deposits of soluble substances such as cytokines released by leukocytes (36). The accumulation and distribution of the macrophages corresponded to these destructive processes.

Leukoencephalopathies occur in small-vessel sporadic (37) and hereditary (38) meningocortical CAAs, Binswanger subcortical vascular encephalopathy (39), cerebral autosomal-dominant arteriopathy with subcortical infarcts

and leukoencephalopathy (40), microangiopathies due to other causes (41), primary angiitis of the CNS, and Aβ-related angiitis (ABRA) (42). The diffuse type of CAA can also be associated with leukoencephalopathy (15, 43).

Unlike cases of ABRA, which have a different type of amyloid deposition and localizations, our case KAB showed a small $CD8^+$ and, to a much lesser extent, $CD4^+$ T-cell infiltration and occasional giant cell reaction. This raises the possibility of a mild autoimmune reaction against amyloid or tissue degradation products. Predominance of infiltrating $CD8^+$ T cells has also been observed in cases of ABRA (44). There was no evidence of a systemic cell-mediated immune disorder, nor was there any iatrogenic influence on the immune system. Thus, these 3 cases, of which patient KAB is the best documented prototype, can be characterized as a novel pathogenetic complex of widespread subcortical vascular amyloidosis with leukoencephalopathy (WSVAL).

One case reported by Lampert (45) had some similarity with these 3 cases; it showed diffuse demyelination of the cerebral hemispheres with a perivascular deposition of an "amyloid-like" but CR-negative (i.e. nonamyloid) substance accompanied by accumulations of lymphocytes and plasma cells. That case seems to represent an as-yet-unknown disease process.

Amyloid Chemistry

Using antibodies directed against different human amyloid proteins, the amyloid peptide was determined to be of λ-light chain origin in cases DU 1 and KAB. Unreliability of antibodies prepared against native λ-light chains has been previously documented (46) and confirmed recently by others (24). Different amyloidotic light chains have antigenic determinants that differ from those of native light chains (24, 47), which might explain the stronger reaction of amyloid KAB with both anti-ALλ antibodies than with anti-λ. As shown here, this amyloid is associated with highly sulfated glycosaminoglycans as is the case for Aβ and other types of amyloid (48).

By partial amino acid sequence analysis, the purified KAB amyloid was found to be an $ALV\lambda_{II}$. The fact that a single amino acid sequence of a particular peptide from the variable region could be identified indicates that this amyloid was produced by a monoclonal plasma cell population.

The Ig isotype differs between the monoclonal immunoglobulin deposition diseases; in systemic ALλ amyloidoses, there is a remarkable overrepresentation of $V\lambda_{VI}$ variable region (49). Interestingly, in addition to case KAB, in 2 of 4 other cases of primary cerebral ALλ amyloidoses (17, 35, 50, 51), there were homologies to subgroup $V\lambda_{II}$ by partial sequence analysis. This remains to be further clarified.

Double-Immunohistochemical Reactivities to Amyloid in Other CAAs

Reaction of more than 1 antibody to a defined amyloid was reported in 1986 (47) and has been confirmed by several groups; this is common to chemically different amyloids and also applies to cerebral amyloid angiopathies (24). It has been reported that λ-immunoreactivity is found in a high percentage in Aβ angiopathy in Alzheimer disease (52, 53) and in nondemented patients (including 3 of 4 of our own unpublished cases). From these findings, however, it would be premature to conclude that 2 different amyloid proteins are deposited as amyloid because it has not been shown that the λ-chain is an integral part of the amyloid fibril, and free λ proteins might be adsorbed to the amyloid from the circulation. If not considered, this can compromise the precise classification based on immunohistochemistry. Indeed, frequent adsorption of cystatin C from the CSF to Aβ type of CAA has been demonstrated by chemical analysis showing that cystatin C was not a component of the amyloid fibril protein (54, 55); the same occurred in cases with giant cell angiitis to Aβ degradation in ABRA in which light chains (56) and cystatin C (57) were detected by immunohistochemistry. In contrast, the amyloid fibril protein in the present case KAB was mainly composed of λ-light chain–derived proteins and had no Aβ or other apparent composition.

Monoclonal Plasma Cells

As in our case KAB, the λ monotype of the local plasma cells was demonstrated by immunohistochemistry in case DU 1 (33). Moreover, only increased λ-light chains, but not κ-light chains, were detected in the CSF in our case KAB This implicates a plasma cell clone in this fatal neuropathology by the production of a single amyloidogenic λ-light chain, but it was not possible to definitively prove their monoclonality by gene rearrangement analysis because intact DNA could not be retrieved from the paraffin blocks probably due to autolysis and prolonged storage.

The absolute numbers of plasma cells may vary greatly; based on semiquantitative data in case DU 1, there were 10 to 20 told plasma cells than in our case (33). T cells and macrophages differed only by a factor of 2 between the cases. The numbers of plasma cells, however, may also vary during disease depending on the balance of their proliferation, apoptosis, and, possibly, emigration. This was suggested in our case because there was a decrease in the amount of the intrathecal IgG synthesis (20) and of free λ-light chain concentration measured over the course of the disease. This might account for very low plasma cell numbers in relation to the massive amyloid deposition in the brain at autopsy and suggests a self-limiting proliferative process of a population that may even decrease with time. In this regard, the T-cell populations, which usually indicate their regulating function of an immunological process, were nearly exclusively $CD8^+$ T cells in case KAB This suggests that the plasma cell clone probably was not dependent on a helper function of $CD4^+$ cells and that it might proliferate in an autonomous manner.

The composition of the plasma cell infiltrates corresponds to what has been termed "atypical monoclonal plasma cell hyperplasia" in 2 cases of a dural process (58, 59). Recently, a 38-year-old female with similar intracerebral perivascular infiltrates, mainly of plasma cells with low proliferative activity involving the white matter but not the cerebral cortex, was reported (60). By immunohistochemistry and gene rearrangement analysis, the cells were shown to be

monoclonal IgGκ type. No amyloid could be detected, whereas CSF immunoglobulin synthesis was high. With respect to the plasma cell infiltration, our case KAB can be classified within this category, that is, a lesion that is neither primarily inflammatory nor obviously malignant but of unknown prognosis if it is not complicated by amyloid formation. The premalignant nature of these cells has been favored (58) but has not been proven. The case mentioned above, described by Lampert (45), also showed atypical intracerebral plasma cell proliferation, but possibly non-amyloidotic immunoglobulin deposition. In our opinion, however, designation of this condition as "atypical monoclonal plasma cell proliferation" instead of "hyperplasia" is preferable in the brain, an organ that normally lacks plasma cells; the monoclonality of these cells leaves their precise identity uncertain. Moreover, the pathogenesis of this autonomous monoclonal plasma cell proliferation, with or without amyloidogenic capability, and an explanation for the strikingly predominant white matter involvement are also unclear.

Preterminal Systemic Monoclonal Gammopathy

Although the concentration of the free λ-light chain in the CSF in case KAB declined during the disease course, there was a remarkable steep increase of the free λ-light chain in serum to a more than 20-fold concentration compared with the CSF one month before death. That suggests that some cells of the λ-clone escaped the brain and found other favorable conditions outside the brain, the sites of which could not be identified. There was, however, a considerable amount of the free λ-light chain found in the circulation, that is, a preterminal monoclonal gammopathy of unspecified source and of undetermined significance. Development of a monoclonal gammopathy of unspecified source and of undetermined significance in this manner has not to our knowledge previously been documented.

Other Diseases With Brain-Restricted AL Amyloid Deposition

There are several AL amyloid deposition diseases that are in the differential diagnosis of WSVAL (Table 4). Twenty-seven cases of tumorlike cerebral amyloid masses originating from confluent perivascular deposits (i.e. amyloidomas) have been reported (61); most of these are located in the white matter. An exclusive ALλ type amyloid was detected biochemically (17, 35, 51) or by immunohistochemistry (62–65). With one exception (35), these amyloid masses were generally associated with only a few mature plasma cells, as in WSVAL. Their monoclonality was shown by gene rearrangement analysis (63). Monoclonal IgGλ and free λ-light chains was also detected n the CSF of 1 patient (34). Despite these similarities with WSVAL and the observation that local confluence to compact amyloid can occur in WSVAL (as in case DU 1), these ALλ deposition diseases are distinguished by their different distributions (local vs widespread), and the evidently more benign course of the disease in most cases of amyloidoma (up to 30 years [51]), and the possibility of surgical resection.

A unique case with exclusively leptomeningeal amyloid angiopathy has to be mentioned (50). Numerous cortical microinfarcts and leukoencephalopathy had arisen by the severe damage of the subarachnoid vessels. The chemically analyzed amyloid yielded an ALλ type, the source of which remained unclear. One may hypothesize that a leptomeningeal plasmacytosis within the 11 years of the clinical course had vanished in the terminal stage.

Solitary intracerebral plasmacytomas are very rare. Only 13 cases have been reported (66–78); only 4 of these showed amyloid formation (68, 70, 75, 76). Although monoclonal in nature, the neoplastic plasma cells obviously produce immunoglobulins that are only partly amyloidogenic. Similarly, extramedullary plasmacytomas (e.g. 4 of 12 cases of solitary dural plasmacytomas) also developed amyloid (79). To date, the type of amyloid in solitary cerebral plasmacytomas has not been shown, but in other organs, an AL type was demonstrated by sequence analysis (80), in agreement with the restriction pattern of the tumor cells.

Primary intracerebral B-cell lymphomas such as lymphoplasmacytic lymphoma, marginal zone lymphoma, and small lymphocytic lymphoma with plasmacytic differentiation would have the potential for amyloid production. This is a very small group within the primary CNS lymphomas, and only 2 cases of amyloid formation within an intracerebral lymphoma have been reported. The first case was a lymphoplasmacytic lymphoma that secreted monoclonal IgGλ into the CSF; the amyloid type was not determined (81). The second case may also be classified as an intracerebral amyloidoma (see previous sentences) and was a lymphoplasmacytic lymphoma with particularly massive, tumefactive amyloid production (35). There was, however, an exceptionally long clinical course of 37 years, and in that case, ALλ amyloid was verified. This constellation might be interpreted as a final lymphomagenesis from an originally very slowly proliferating local plasma cell clone with massive amyloid accumulation, as in other amyloidomas. The distinction between CNS amyloidoma from lymphoma with amyloid deposition in an individual case is a difficult diagnostic problem, as in other organs (82).

Local vascular amyloid deposition can occur in other pathogenetic conditions, in chronic demyelinating MS lesions, with 6 cases reported (83, 84). This amyloid was characterized by immunohistochemistry as ALλ (85). In the area of the lesions, there are perivascular mature plasma cells with restricted λ-light chain expression; monoclonality was shown by gene rearrangement analysis (84). Thus, in these cases, monoclonal plasma cells synthesize and excrete

TABLE 4. Diseases With Brain-Restricted AL-Type Amyloid Deposition

Amyloidoma
Widespread subcortical vascular amyloidosis with leukoencephalopathy (this paper)
Leptomeningeal vascular amyloidosis
Solitary intracerebral plasmacytoma
Primary intracerebral B-cell lymphoma with plasmacytic differentiation
Multiple sclerosis with demyelination associated amyloid deposition

immunoglobulin λ-light chains that can give rise to amyloid at the vascular walls. We postulate, therefore, that, as may occur in other autoimmune inflammatory diseases (86), an autonomously expanding monoclonal plasma cell clone can be established from the originally polyclonal inflammatory B-cell populations by escaping T-cell regulation. The special conditions required for this transition in these rare cases remain to be determined.

In conclusion, there are different pathologic constellations associated with cerebral vessel–bound amyloid deposits originating from immunoglobulin light chains. So far, only ALλ has been verified in many examined cases. The precursor proteins are synthesized and secreted by a singular autonomous plasma cell clone that has a very limited proliferative potential in cases of amyloidoma, WSVAL, leptomeningeal amyloid angiopathy, and MS with amyloid formation. In plasmacytoma and other lymphomas, by contrast, their malignant neoplastic character is obvious. The amyloidogenic potency seems to be very different, possibly depending on the degree of the differentiation of the plasma cells and the chemistry of their product. We show here that the new entity WSVAL is a special type within this group of diseases with subcortical predilection that results from excessive immunoglobulin light chain production of a disseminated perivascular small plasma cell clone, which seems to have no obvious primary malignant features. The fatal prognosis is due to its amyloidogenic secretion product that leads to very widespread severe angiopathic changes within the brain.

ACKNOWLEDGMENTS

The authors thank Irmgard Henke, Renate Kott (both from Cologne), and Rosl Oos, Reinhild Joswig, and Johanna Lindermayer (all from Martinsried) for excellent technical assistance. The free light chain quantification was performed by Dr. Markus Zorn, Central Laboratory, University of Heidelberg, Germany. Reinhard Mentele and Dr. Joseph Kellermann performed the amino acid sequence analysis of the amyloid peptide. The laboratory space for these investigations was kindly provided by Prof. Dr. Robert Huber, all Max-Planck-Institute of Biochemistry, Martinsried. Drs. Manuel Hermann and Werner Stenzel (Cologne) assisted with electronic preparation of the figures. Special thanks are directed to Prof. Dr. Rudolf Ackermann, formerly Neurological Clinic, University Hospital of Cologne, who stored the patient's CSF and serum samples and autopsy brain tissue for years and provided them for examinations. This article is dedicated to Prof. emer. Dr. Lieselotte Gerhard, University of Essen, Germany.

REFERENCES

1. Castaño EM, Frangione B. Biology of disease. Human amyloidosis, Alzheimer disease and related disorders. Lab Invest 1988;58:122–32
2. Glenner GG, Murphy MA. Amyloidosis of the nervous system. J Neurol Sci 1989;94:1–28
3. Haan J, Roos RAC. Amyloid in central nervous system disease. Clin Neurol Neurosurg 1990;92:305–10
4. Castaño EM, Frangione B. Non-Alzheimer's disease amyloidoses of the nervous system. Curr Opin Neurol 1995;8:279–85
5. Revesz T, Ghiso J, Lashley T, et al. Cerebral amyloid angiopathies: A pathologic, biochemical and genetic view. J Neuropathol Exp Neurol 2003;62:885–98
6. Ishihara T, Nagasawa T, Yokota T, et al. Amyloid protein of vessels in leptomeninges, cortices, choroid plexuses, and pituitary glands from patients with systemic amyloidosis. Human Pathol 1989;20: 891–95
7. Schröder R, Linke RP. Cerebrovascular involvement in systemic AA and AL amyloidoses: A clear haematogenic pattern. Virchows Arch 1999; 434:551–60
8. Gerhard L, Bergener M, Homayun S. Angiopathie bei Alzheimerscher Krankheit. Z Neurol 1972;201:43–61
9. Vinters HV. Cerebral amyloid angiopathy. A critical review. Stroke 1987;18:311–24
10. Thal DR, Ghebremedhin E, Orantes M, Wiestler O. Vascular pathology in Alzheimer disease: Correlation of cerebral amyloid angiopathy and arteriosclerosis/ lipohyalinosis with cognitive decline. J Neuropathol Exp Neurol 2003;62:1287–301
11. Ghetti B, Piccardo P, Spillantini MG, et al. Vascular variant of prion protein cerebral amyloidosis with τ-positive neurofibrillary tangles. The phenotype of the stop codon 145 mutation in *PRNP*. Proc Natl Acad Sci U S A 1996;93:744–48
12. Kiuru S, Salonen O, Haltia M. Gelsolin-related spinal and cerebral amyloid angiopathy. Ann Neurol 1999;45:305–11
13. Holton JL, Ghiso J, Lashley T, et al. Regional distribution of amyloid-Bri deposition and its association with neurofibrillary degeneration in Familial British dementia. Am J Pathol 2001;158: 515–26
14. Holton JL, Lashley T, Ghiso J, et al. Familial Danish dementia: A novel form of cerebral amyloidosis associated with deposition of both amyloid-Dan and amyloid-beta. J Neuropathol Exp Neurol 2002;61: 254–67
15. Shaw C-M. Primary idiopathic cerebrovascular amyloidosis in a child. Brain 1979;102:177–92
16. Ushiyama M, Ikeda S, Yanagisawa N. Transthyretin-type cerebral amyloid angiopathy in type I familial amyloid polyneuropathy. Acta Neuropathol 1991;81:524–28
17. Vidal RG, Ghiso J, Gallo G, et al. Amyloidoma of the CNS. II. Immunohistochemical and biochemical study. Neurology 1992;42: 2024–28
18. Peters G. Paraproteinosen und Zentralnervensystem. Dtsch Z Nervenheilk 1949;161:359–95
19. Peters G. Über Paramyloidose des Gehirns. Verh Dtsch Ges Pathol 1950;32:83–89
20. Erkwoh R, Schröder R, Ackermann R. Eine ungewöhnliche zerebrovaskuläre Amyloidose mit dem klinischen Bild einer chronischen Enzephalitis. Nervenarzt 1987;58:311–16
21. Puchtler H, Sweat F, Levine M. On the binding of Congo red by amyloid. J Histochem Cytochem 1962;10:355–64
22. Scott JE, Dorling J. Differential staining of acid glycosaminoglycans (mucopolysaccharides) by Alcian blue in salt solutions. Histochemie 1965;5:221–33
23. Linke RP. Highly sensitive diagnosis of amyloid and various amyloid syndromes using Congo red fluorescence. Virchows Arch Pathol Anat 2000;436:439–48
24. Linke RP. Congo red staining of amyloid. Improvements and practical guide for a more precise diagnosis of amyloid and the different amyloidoses. In: Uversky VN, Fink AL, eds. *Protein Misfolding, Aggregation and Conformational Diseases. Protein Reviews 2006 Vol. 4 (MZ Atassi, ed.); Chapter 11.1*. Heidelberg, Germany:Springer, 239–76
25. Linke RP, Oos R, Wiegel NM, Nathrath WBJ. Classification of amyloidosis: Misdiagnosing by way of incomplete immunohistochemistry and how to prevent it. Acta Histochem 2006;108:197–208
26. Linke RP. Immunohistochemical typing of amyloid deposits after microextraction from biopsies. Appl Pathol 1985;3:18–28
27. Laemmli LK. Cleavage of structural proteins during the assembly of the head of bacteriophage T4. Nature 1970;227:680–85
28. Towbin H, Staehelin T, Gordon G. Electrophoretic transfer of proteins and some applications. Proc Natl Acad Sci U S A 1979;76:4350–54
29. Lottspeich F. Proteinsequenzanalyse. In: Lottspeich F, Engels JW, eds. *Bioanalytik*. München: Elsevier-Spektrum, 2006:311–28

30. Schröder R. *Chronomorphologie der zerebralen Durchblutungsstörungen. Schriftenreihe Neurologie*, vol. 24. Heidelberg, Germany: Springer, 1983:88–93
31. Kohler H, Rudolfsky S, Kluskens L. The primary structure of a human lambda II chain. J Immunol 1975;114:415–21
32. Gerhard L. Ein Fall von Amyloidose des Gehirns (Abstract). Zentrbl allg Pathol 1959;100:282
33. Yuan Y. *Zwei Fälle von Markgefäß-Amyloidose des Gehirns*. Essen, Germany: Medical Dissertation, University of Essen, 1996
34. Cohen M, Lanska D, Roessmann U, et al. Amyloidoma of the CNS. I. Clinical and pathologic study. Neurology 1992;42:2019–23
35. Linke RP, Gerhard L, Lottspeich F. Brain-restricted amyloidoma of immunoglobulin λ-light chain origin clinically resembling multiple sclerosis. Biol Chem Hoppe-Seyler 1992;373:1201–9
36. Weller RO, Subash M, Preston SD, et al. Perivascular drainage of amyloid-β peptides from the brain and its failure in cerebral amyloid angiopathy and Alzheimer's disease. Brain Pathol 2008;18: 253–66
37. Yoshimura M, Yamanouchi H, Kuzuhara S, et al. Dementia in cerebral amyloid angiopathy: A clinicopathological study. J Neurol 1992;239: 441–50
38. Haan J, Algra PR, Roos RAC. Hereditary cerebral hemorrhage with amyloidosis–Dutch type. Clinical and computed tomographic findings of 24 cases. Arch Neurol 1990;47:649–53
39. Fisher CM. Binswanger's encephalopathy: A review. J Neurol 1989;236: 65–69
40. Ruchoux MM, Maurage CA. CADASIL: Cerebral autosomal dominant arteriopathy with subcortical infarcts and leukoencephalopathy. J Neuropathol Exp Neurol 1997;56:947–64
41. Zu Rhein GM, Lo S-C, Hulette CM, Powers JM. A novel cerebral microangiopathy with endothelial cell atypia and multifocal white matter lesions: A direct mycoplasma infection? J Neuropathol Exp Neurol 2007;66:1100–17
42. Scolding NJ, Joseph F, Kirby PA, et al. Aβ-related angiitis: Primary angiitis of the central nervous system associated with cerebral amyloid angiopathy. Brain 2005;128:500–15
43. Plant GT, Révész T, Barnard RO, et al. Familial cerebral amyloid angiopathy with nonneuritic amyloid plaque formation. Brain 1990;113: 721–47
44. Yamada M, Yoshinori I, Shintaku M, et al. Immune reactions associated with cerebral amyloid angiopathy. Stroke 1996;27:1155–62
45. Lampert PW. Amyloid and amyloid-like deposits. In: Minckler J, ed. *Pathology of the Nervous System*, vol 1. New York: McGraw-Hill, 1968: 1113–21
46. Chastonay P, Hurlimann J. Characterization of different amyloids with immunological techniques. Pathol Res Pract 1986;181:657–63
47. Platz SJ, Breuer W, Geisel O, et al. Identification of lambda light chain amyloid in eight canine and two feline extramedullary plasmacytomas. J Comp Pathol 1997;116:45–54
48. Snow AD, Mar H, Nochlin D, et al. The presence of heparan sulfate proteoglycans in the neuritic plaques and congophilic angiopathy in Alzheimer's disease. Am J Pathol 1988;133:456–63
49. Solomon A, Frangione B, Franklin EC. Bence Jones proteins and light chains of immunoglobulins preferential association of the $V_{\lambda VI}$ subgroup of human light chains with amyloidosis AL(λ). J Clin Invest 1982;70: 453–60
50. Layfield R, Bailey K, Lowe J, et al. Extraction and protein sequencing of immunoglobulin light chain from formalin-fixed cerebrovascular amyloid deposits. J Pathol 1996;180:455–59
51. Eriksson L, Sletten K, Benson L, Westermark P. Tumor-like localized amyloid of the brain is derived from immunoglobulin light chain. Scand J Immunol 1993;37:623–26
52. Kametani F, Tanaka K, Sato M, et al. A monoclonal antibody Hy20-54-16-3 L to lambda (λ) light chain of human immunoglobulin reacts with amyloid in Alzheimer's disease brain. Neurosci Lett 1990;117: 62–67
53. Linke RP, Schifferegger R, Kretschmar H, Gerhard L. Antigenic heterogeneity of cerebral amyloid deposits in Alzheimer's disease. In: Natvig JB, Førre Ø, Husby G, et al. eds. *Amyloid and Amyloidosis*. *VIth Int Symposium on Amyloidosis*. Dordrecht, The Netherlands: Kluwer Academic Publ, 1991;741–44
54. Maruyama K, Ikeda S, Ishihara T, et al. Immunohistochemical characterization of cerebrovascular amyloid in 46 autopsied cases using antibodies to β protein and cystatin C. Stroke 1990;21:397–403
55. Maruyama K, Kametani F, Ikeda S, et al. Characterization of amyloid fibril protein from a case of cerebral amyloid angiopathy showing immunohistochemical reactivity for both beta protein and cystatin C. Neurosci Lett 1992;144:38–42
56. Murphy MN, Sima AAF. Cerebral amyloid angiopathy associated with giant cell arteritis: A case report. Stroke 1985;16:514–17
57. Anders KH, Wang ZZ, Kornfeld M, et al. Giant cell arteritis in association with cerebral amyloid angiopathy: Immunohistochemical and molecular studies. Hum Pathol 1997;28:1237–46
58. Weidenheim KM, Campbell WG, Goldman HW. Atypical monoclonal plasma cell hyperplasia of the central nervous system: Precursor of plasmacytoma with evolutionary considerations. Neurosurgery 1989;24: 429–34
59. Hsiang JNK, Ho-Keung N, Wai-Sang P. Atypical monoclonal plasma cell hyperplasia: Its identity and treatment. Case report. J Neurosurg 1996;85:697–700
60. Viehöver A, Hähnel S, Weber M-A, et al. Atypische monoklonale Plasmazellhyperplasie. Infiltration des ZNS. Nervenarzt 2006;77: 1495–500
61. Fischer B, Palkovic S, Rickert C, et al. Cerebral AL lambda-amyloidoma. Review of the literature and of a patient. Amyloid 2007;14:11–19
62. Schröder R, Linke RP, Voges J, et al. Intracerebral ALλ amyloidoma diagnosed by stereotactic biopsy. Clin Neuropathol 1995;14:347–50
63. Laeng RH, Altermatt HJ, Scheithauer BW, Zimmermann DR. Amyloidomas of the nervous system. A monoclonal B-cell disorder with monotypic amyloid light chain λ amyloid production. Cancer 1998;82: 362–74
64. Meir K, Maly B, Shoshan Y, et al. Cerebral amyloidoma diagnosed intraoperatively with squash preparations: A case report. Acta Cytol 2005;49:195–98
65. Tabatabai G, Baehring J, Hochberg FH. Primary amyloidoma of the brain parenchyma. Arch Neurol 2005;62:477–80
66. French JD. Plasmacytoma of the hypothalamus. Clinical-pathological report of a case. J Neuropathol Exp Neurol 1947;6:265–70
67. Castleman B, Scully RE, McNeely BU. Case records of the Massachusetts General Hospital. Weekly clinicopathological exercises. Case 3–1973. N Engl J Med 1973;288:150–56
68. Goryachkina GP. Solitary plasmacytoma of the hypothalamus (in Russian). Arkh Patol 1979;41:53–57
69. Kanie N, Banno T, Shibuya M, et al. Solitary intracerebral plasmacytoma. Neurol Med Chir (Tokyo) 1981;21:337–43
70. Krumholz A, Weiss HD, Jiji VH, et al. Solitary intracerebral plasmacytoma: Two patients with extended follow-up. Ann Neurol 1982;11: 529–32
71. Husain MM, Metzer WS, Binet EF. Multiple intraparenchymal brain plasmacytoma with spontaneous intratumoral hemorrhage. Neurosurgery 1987;20:619–23
72. Cvetković D, Dožić S, Samardžić M, et al. Solitary cerebral plasmacytoma—Report of a case (Abstract). Clin Neuropathol 1989;8:224
73. Wisniewski T, Sisti M, Inhirami G, et al. Intracerebral solitary plasmacytoma. Neurosurgery 1990;27:826–29
74. Inbasekaran V, Vijayarathinam P, Arumugam S. Solitary intracerebral plasmacytoma. J Indian Med Assoc 1991;89:16–17
75. Rivas L, Guzmán JR, Mora-La Cruz E, Cardozo J. Plasmocitoma solitario intracraneal extramedular: Reporte de dos casos. Invest Clin 1994;35:155–67
76. Suna D, Erdinçler P, Bayindir Ç, et al. Plasmocytome solitaire intracérébral. À propos d'un cas peut-être induit par un trauma crânien. Neurochirurgie 1997;43:255–59
77. N'Dri OD, Varlet G, Koffi G, et al. Plasmocytome solitaire intracérébral. À propos d'un cas peut-être induit par un traumatisme crânien. Neurochirurgie 2000;46:401
78. Hayes-Lattin B, Blanke CD, Deloughery TG. Pulmonary and intracerebral plasmacytomas in a patient without multiple myeloma: A case report. Am J Hematol 2003;73:131–14
79. Mancardi GL, Mandybur TI. Solitary intracranial plasmacytoma. Cancer 1983;51:2226–33

80. Röcken C, Hegenbarth V, Schmitz M, et al. Plasmacytoma of the tonsil with AL amyloidosis: Evidence of postfibrillogenic proteolysis of the fibril protein. Virchows Arch 2000;436:336–44
81. Ellie E, Vergier B, Duche B, et al. Local amyloid deposits in a primary central nervous system lymphoma. Study of a stereotactic biopsy. Clin Neuropathol 1990;9:231–33
82. Dacic S, Colby TV, Yousem SA. Nodular amyloidoma and primary pulmonary lymphoma with amyloid production: A differential diagnostic problem. Mod Pathol 2000;13:934–40
83. Heffner RR, Porro RS, Olson ME, Earle KM. A demyelinating disorder associated with cerebrovascular amyloid angiopathy. Arch Neurol 1976; 33:501–6
84. Nennesmo I, Bogdanovic N, Petrén A-L, Fredrikson S. Multiple sclerosis and amyloid deposits in the white matter of the brain. Acta Neuropathol 1997;93:205–9
85. Schröder R, Nennesmo I, Linke RP. Amyloid in a multiple sclerosis lesion is clearly of Aλ type. Acta Neuropathol 2000;100:709–11
86. Santana V, Rose NR. Neoplastic lymphoproliferation in autoimmune disease: An updated review. Clin Immunol Immunopathol 1992;63: 205–13

